

2102-97- 205941

FINAL
IN-24-11
O.C.T.
082355

**Performance Enhancement of a High Speed Jet
Impingement System for Nonvolatile Residue Removal**

Final Report

Grant Number: NAG10-0177

September 5, 1995 to December 15, 1996

Technical Contact: Greg Melton

Materials Science Laboratory

DM-MSL-21

Kennedy Space Center

KSC, Florida 32899

Principal Investigators: James F. Klausner and Renwei Mei

Research Assistants: Steve Near and Rex Stith

University of Florida

Gainesville, Florida 32611

Table of Contents

1 Introduction	2
2 Physical Considerations of High Velocity Jet Impingement Systems	5
2.1 Flow Structure	5
2.2 An Analogy with Particle Impact Erosion	8
2.3 Theoretical Framework for Residue Removal	9
3 Experimental Apparatus and Instrumentation	12
3.1 Description of High Speed Jet Impingement Facility	12
3.2 Description of Instrumentation	20
3.3 Reflectivity Calibration and Residue Measurement Protocol	21
3.4 Protocol for Operating High Speed Jet Impingement Facility	25
4 Experimental Results and Discussion	29
5 Conclusions	40
6 References	43
7 Nomenclature	45

List of Figures

- Figure 1 Simple Schematic Diagram of a High Speed Jet Impingement Facility.
- Figure 2a Schematic Diagram of an Under-Expanded Supersonic Jet Normally Impinging a Flat Plate ($\theta=0$).
- Figure 2b Shock Structure of an Under-Expanded Supersonic Jet Impinging an Inclined Flat Plate ($\theta>0$).
- Figure 3 Detailed Schematic Diagram of High Speed Jet Impingement Facility.
- Figures 4a-d Detailed Drawings of Mixing Chamber and Orifice Adapters.
- Figure 5a Conventional Converging-Diverging Nozzle.
- Figure 5b Annular Converging-Diverging Nozzle.
- Figure 6 Experimental Alignment for Laser Reflectivity Residue Measurement.
- Figure 7 Calibration Curve for Residue Contamination Using Laser Reflectivity.
- Figure 8 Residue Removal Rate as a Function of Nozzle Distance to Cleaning Surface (Conventional Converging-Diverging Nozzle, 15° Approach Angle, No Heating).
- Figure 9 Residue Removal Rate as a Function of Nozzle Distance to Cleaning Surface (Annular Converging-Diverging Nozzle, 15° Approach Angle, No Heating).
- Figure 10 Residue Removal Rate as a Function of Water Temperature (Annular Converging-Diverging Nozzle, 15° Approach Angle, 1" Nozzle Distance).
- Figure 11 Residue Removal Rate as a Function of Mixture Temperature (Annular Converging-Diverging Nozzle, 15° Approach Angle, 3/4" Nozzle Distance).
- Figure 12 Water Flow Rate as a Function of Mixing Chamber Temperature (0.016" Orifice).

1 Introduction

The cleaning of aerospace systems and components is essential for the safe, efficient, and reliable operation of advanced aircraft and space transport vehicles. Strict cleanliness requirements are especially important for liquid oxygen (LO_2) systems which are routinely serviced at NASA Kennedy Space Center (KSC). Historically, the aerospace industry has heavily relied upon trichlorotrifluoroethane (R113) and other chlorofluorocarbon (CFC) fluids to remove organic and nonorganic residues due to their excellent solvency potential. KSC processes approximately 250,000 pieces through the component cleaning facility per year (Littlefield et al., 1994). Of these, approximately 1000 pieces are classified as large components and the remaining pieces are classified as small components. During 1993 60,000 pounds of R113 were consumed for cleaning and verification purposes. However, due to the suggested destruction of the upper ozone layer from the release of CFC compounds, they have been phased out of production since January, 1996. Currently, ultrasonic water baths are successfully utilized to clean small parts (Melton et al., 1993). However, there remains uncertainty as to the most effective means of cleaning large components which consist of valves, regulators, pipes, k-bottles, flexible hose lines, and others.

Apart from the cleaning difficulties encountered at NASA KSC, the entire aerospace industry faces similar challenges. For example, due to the high temperatures encountered in military jet afterburners, perfluorinated polyether (PTFE) greases are used for lubrication purposes, but they are chemically inert and very difficult to remove during inspection and repair. After studying a variety of cleaning options, Thom (1995) found that

hydrofluorocarbon (HFC) solvents in conjunction with ultrasonic baths yielded the best performance. The cleaning of compressor blades in advanced aircraft engines has also been a concern. Kolkman (1993) has tested four new commercially available cleansers which are reported to be "ecologically sound." Of the new cleansers tested, all were found to have poor performance compared with those that have previously been used in practice. Hills (1995) has studied the performance of CO₂ jet sprays in removing organic compounds from solid surfaces. During the operation of this cleaning facility, CO₂ is expanded through an orifice so that a gas/solid mixture is formed. The mixture then flows through a nozzle which controls the solid particle size. It was found that the jet spray was effective in cleaning certain organic compounds and not others. The contaminants which had the greatest solubility in liquid CO₂ were most effectively removed. It was thus hypothesized that cleaning occurs due to both abrasion and solvency.

Due to the growing demand for non-ozone depleting solvents, 3M Engineering has been developing hydrofluoroethers as replacements. The solvent HFE-A (C₄F₉OCH₃) is reported (Morkid, 1995) to have zero ozone depletion potential with very similar properties to R113. However, such solvents are expensive compared to the price of CFC's before they were phased out of production.

Currently the surface cleanliness requirement is that there can be no more than 11.1 mg/m² of NVR. In order to address the problem of cleaning large aerospace systems and components, the NASA KSC Material Science Laboratory has developed a high velocity breathing air/water jet impingement system which has been demonstrated to be useful in the cleaning and verification of the nonvolatile residue (NVR) requirement (Dearing et al.,

1993). A description of the experimental facility and design procedure are given by Caimi and Thaxton (1993). The jet impingement facility developed at NASA KSC has the advantage over conventional high speed water jets in that the amount of water consumed is extremely low, typically 30-40 ml/min. Thus, the disposal of the waste water is greatly simplified.

Although the jet impingement facility has been successful in removing nonvolatile residues, the primary mechanism responsible for residue removal is not well understood. When the air stream is maintained at low temperatures, it has been observed that liquid droplets discharging from the nozzle solidify and ice crystals impact the cleaning surface. Under such an operating condition it is possible for residue to be removed due to abrasion of the crystals or through liquid emulsification of the residue upon impact. When the droplets remain in a liquid state it is hypothesized that the cleaning mechanism is due to emulsification.

The primary objective of the research described in this report is to fabricate an experimental high speed jet impingement facility and characterize its effectiveness in removing nonvolatile residues over a range of operating conditions with different nozzle configurations. It is desired to determine the optimum operating condition. It is anticipated that these tests will also provide some fundamental insight into the most effective residue removal mechanism.

2 Physical Considerations of High Velocity Jet Impingement Systems

2.1 Flow Structure

A typical high speed jet impingement cleaning system is shown schematically in Figure 1. A high pressure air stream containing suspended liquid droplets expands through a converging-diverging nozzle. The mixture exiting the nozzle impacts the cleaning surface at some appropriate approach angle. The high velocity droplets or ice crystals impact the surface and the kinetic energy is used to remove the surface residue.

The structure of a supersonic jet impinging on an inclined flat plate is extremely complicated even without the presence of the droplets. Since the motions of the droplets will be dictated by the carrier gas flow, it is important to understand the complex flow structures involved. After exiting the nozzle, the flow is typically characterized by many discontinuities, such as barrel shock, exhaust gas jet boundary, Mach disk, reflected shock, plate shock, subtail shock, contact surface, and sometimes a stagnation circulation region. The jet structure is three dimensional and severely distorted near the inclined impingement plate (Lamont and Hunt, 1980; Tsuboi et al., 1991; and Kim and Chang, 1994) as sketched in Figures 2a and 2b. In particular, the maximum wall pressure was found to be several times larger on the inclined plate than the normal plate, which is not intuitively obvious. It is highly unlikely that the flow field between the nozzle and the plate can be described reliably in an analytical manner.

Depending on the inlet temperature of the mixture to the nozzle, it is possible for the gas phase to fall below the freezing temperature of the liquid ($T_f=273^\circ\text{K}$ for water at one atmosphere) upon expansion through the nozzle. Due to heat transfer, it is possible for a

Figure 1 Simple Schematic Diagram of a High Speed Jet Impingement Facility.

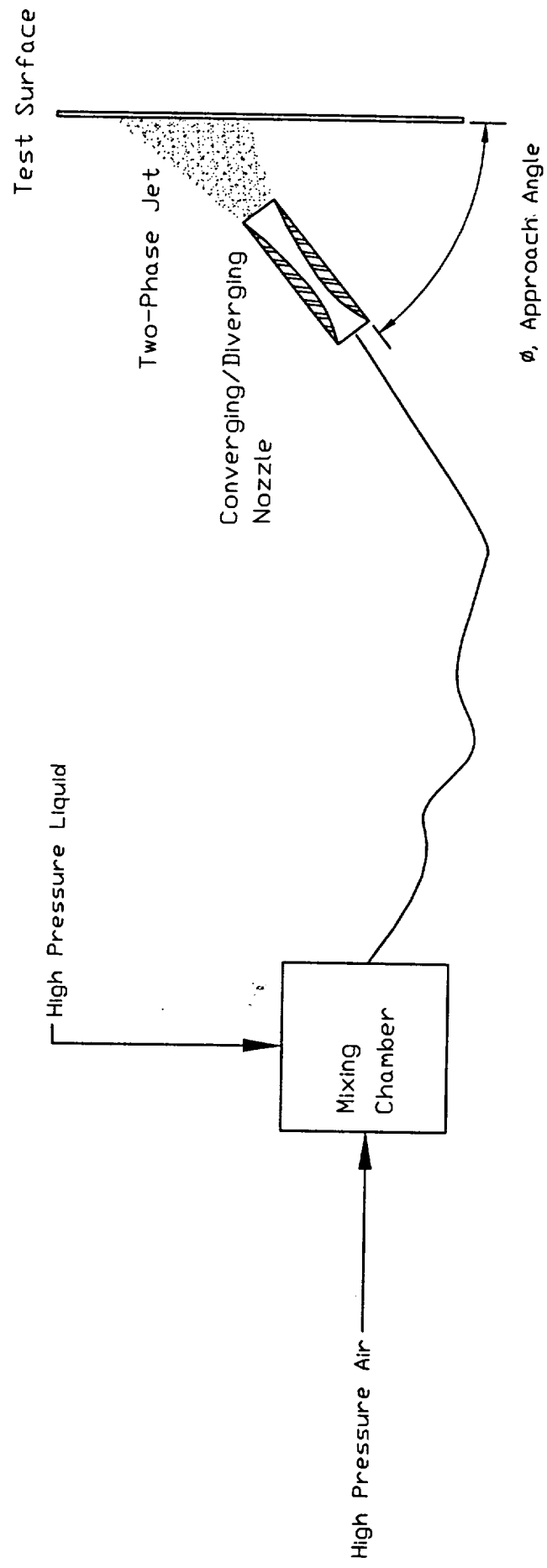


Figure 2a Schematic Diagram of an Under-Expanded Supersonic Jet Normally Impinging a Flat Plate ($\theta=0$).

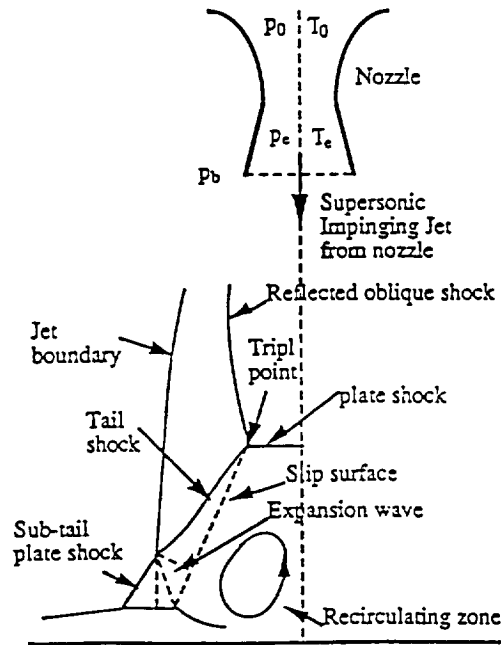
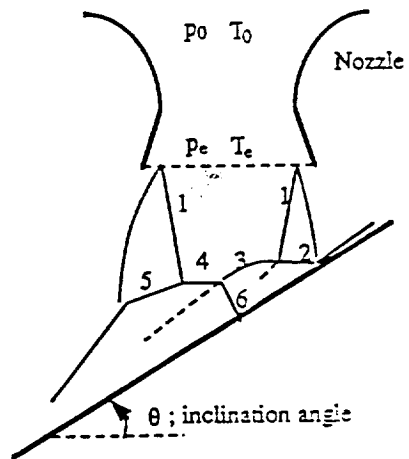


Figure 2b Shock Structure of an Under-Expanded Supersonic Jet Impinging an Inclined Flat Plate ($\theta > 0$).



- 1: jet shock; 2: upper tail shock;
 3: upper plate shock;
 4: lower plate shock; 5: lower tail shock;
 6: intermediate tail shock.

droplet to fall below T_f during its motion toward the impingement plate. The thermal relaxation time may be roughly estimated as $\tau \sim 6k/(a^2\rho_p c_p)$ where k is the thermal conductivity of the gas, a is the droplet radius, ρ_p is the droplet density, and c_p is the droplet heat capacity. This relaxation time is the time required for the droplet to achieve thermal equilibrium with the gas. It is seen that the relaxation time strongly depends on the droplet radius. Thus, smaller droplets have a greater potential to solidify. The solidification process will subsequently follow after the freezing temperature, T_f , is reached during the droplet motion. Typically, the one-dimensional solidification front moves as $s \sim \sqrt{\alpha_s t}$ in which α_s is the solid thermal diffusivity. Due to the extremely high speed at which droplets translate and the relatively short distance they travel prior to striking the plate, the droplets may only partially solidify at the time of surface impact. Thus, the liquid contained within the solidified portion of the droplet can emulsify the surface residue. During operating conditions in which droplets solidify, the degree of solidification may be important in the removal of surface residues.

2.2 An Analogy with Particle Impact Erosion

Although the problem of liquid droplet impingement is different from particle impact erosion which occurs in pneumatic transport systems, the mechanism controlling particle impact erosion can provide some insight into the nonvolatile residue removal mechanism. Most pneumatic transport systems are constructed from ductile metals, and many experimental results have indicated that the erosion rate (i.e. the rate at which mass or volume of the target material is removed) is highest when the particle impact angle, θ (with

respect to the impingement wall) is around 15 to 20 degrees. Finnie (1972) listed factors which may influence the ductile erosion due to particles colliding with the target metal surface: impact angle, rotation of particles, particle velocity at impact, particle size, surface properties, shape of the surface, stress distribution in the surface, particle shape and strength, particle concentration in the fluid stream, and the nature of the carrier gas. By treating an impacting particle as an idealized rigid abrasive particle cutting the target surface, a relation for the eroded volume, V , was derived (Finnie, 1972). The eroded volume was found to be proportional to U^2 in which U is the particle velocity upon impact. Interestingly, the maximum erosion rate occurs when the particle impacts the wall at $\theta \sim 15^\circ$.

Hoff et al. (1966) studied the erosion of solid surfaces due to liquid droplet impact. It was found that the droplet velocity, impact angle, droplet size, and temperature were all important factors in liquid droplet erosion. It was concluded that only the velocity component normal to the surface contributed to droplet erosion. However, in this case the impact droplet is soft while the target material is hard.

2.3 Theoretical Framework for Residue Removal

In cleaning applications, when the stream of impacting droplets remain in a liquid state, the kinetic energy of the droplets are transmitted to the residue to break cohesive and adhesive bonds, resulting in emulsification of the surface residue with the liquid. When the droplets have solidified, the particles will be abrasive and the cutting action of the high speed abrasive ice crystals must break the cohesive and adhesive bonds of the residue.

In carrying through the analogy of jet impingement residue removal with particle or

droplet impact erosion, an energy balance may be used to gain some qualitative insight into parameters influencing the residue removal process. The rate of liquid droplet kinetic energy discharging from the nozzle may be expressed as,

$$\dot{m}_t \frac{U^2}{2} \quad (1)$$

where \dot{m}_t is the liquid mass flow rate through the nozzle and U is the droplet discharge velocity from the nozzle. Only a fraction of the kinetic energy of the droplets leaving the nozzle will contribute to the residue removal upon striking the surface. This fraction will be referred to as the energy utilization parameter and will be designated by ϕ . It is anticipated that ϕ will strongly depend on many different parameters, some of which include the jet approach angle with respect to the cleaning surface, the detailed structure of shock waves the droplets must pass through prior to impacting the cleaning surface, the size of the droplets, the concentration of droplets impacting the surface, and viscosity of the liquid.

The amount of energy required to emulsify a given amount of residue with surface area A_r , is

$$2\sigma_{tr}A_r \quad (2)$$

where σ_{tr} is the interfacial tension between the liquid and residue. For simplicity sake it is assumed that only residue-residue intermolecular forces must be overcome to remove the residue. This implies that only cohesive forces are important. It is recognized that adhesion forces due to residue-solid contact must be overcome to completely remove all of

the residue from the cleaning surface. However, the monolayer of residue in contact with the surface is typically a small fraction of the total residue which must be removed.

Assuming the emulsified residue takes the form of microspheres in the liquid with radius a_r , an energy balance between the rate of kinetic energy available for emulsification and the rate of energy required to emulsify a given amount of material per unit time gives,

$$\dot{m}_t \frac{U^2}{2} \phi = \dot{m}_r \frac{6\sigma_{tr}}{a_r \rho_r} \quad (3)$$

where \dot{m}_r is the mass rate of removal of residue from the cleaning surface and ρ_r is the material density of the residue. Thus it is readily seen that,

$$\dot{m}_r \propto \phi \frac{\dot{m}_t U^2}{\sigma_{tr}} a_r \rho_r \quad (4)$$

A couple of observations from Eq. (4) are worth noting. First, it is seen that the removal of residue depends strongly on the mass flow rate of liquid impinging the surface and the droplet velocity. However, increasing the mass flow rate alone will not necessarily increase the rate of residue removal. The reason is that as the gas/liquid mixture enters the nozzle, the shearing action through the nozzle significantly atomizes the liquid into fine droplets. The smaller the droplet sizes, it is more likely that the droplets will follow the carrier fluid and achieve a high nozzle exit velocity. However, if the mass flow rate of liquid through the nozzle is too great, the liquid will agglomerate into larger droplets and

will be less likely to follow the carrier fluid which will result in lower impact velocities.

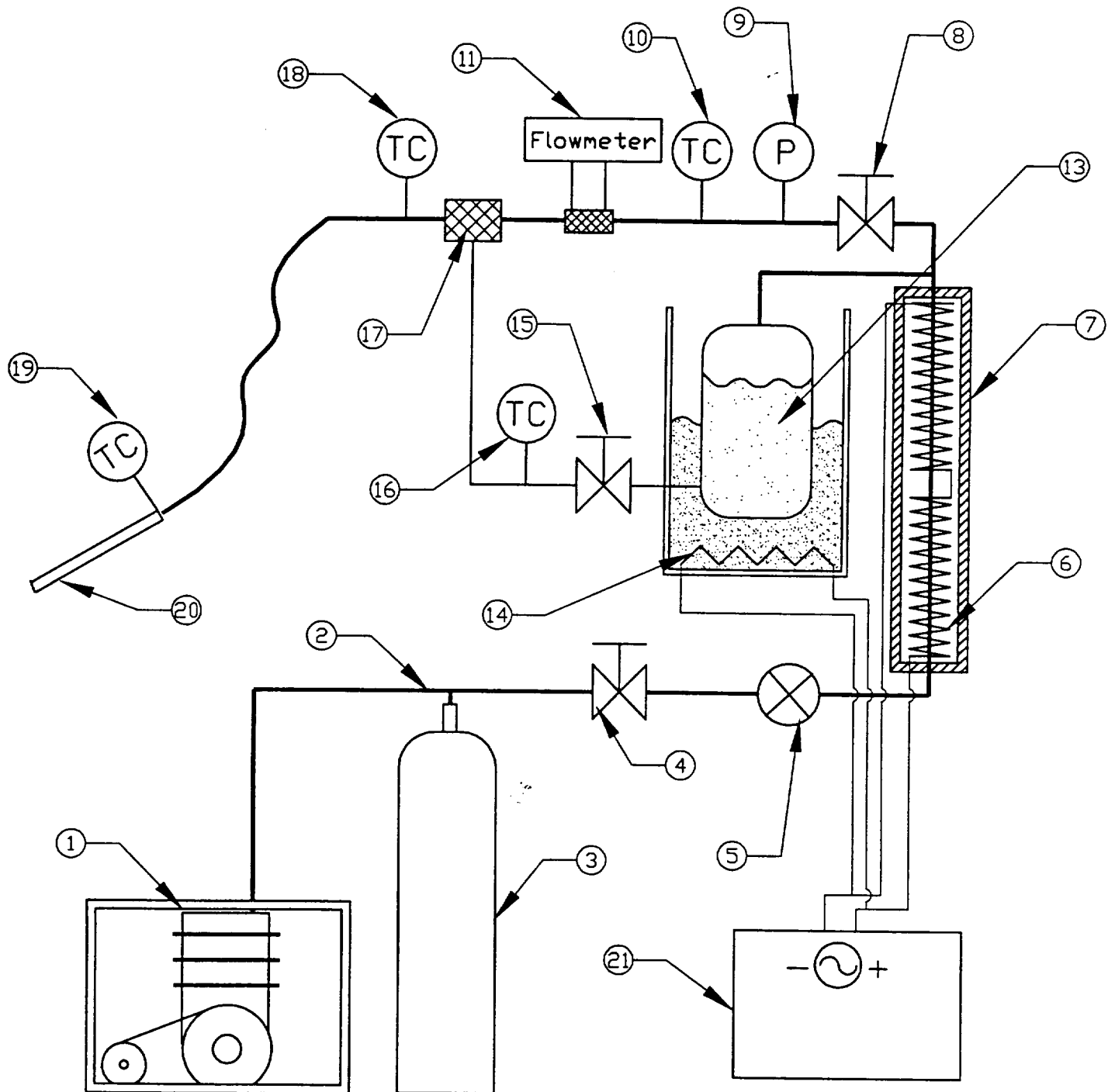
Second, it is seen that the rate of residue removal is inversely proportional to the interfacial tension between the liquid and residue. Since interfacial tension is typically inversely proportional to temperature, Eq. (4) predicts that the rate of residue removal due to emulsification will be enhanced with increasing temperature. Low temperature operation of the system may appear to be attractive since the ice formation can enhance the abrasive residue removal. However, the cohesive strength of the residue is increased at low temperatures and could offset any gains realized from abrasive impact. These considerations must be tested experimentally. As has already been mentioned, the energy utilization parameter, ϕ , depends on many different variables in the operating system, and can only be determined experimentally.

3 Experimental Apparatus and Instrumentation

3.1 Description of High Speed Jet Impingement Facility

An experimental high speed jet impingement facility was fabricated in order to characterize the effectiveness in removing nonvolatile residues over a range of operating conditions. A schematic diagram of the facility is depicted in Figure 3 with an attached parts list. The facility was designed to operate in the batch mode because it was desired to bring the air temperature expanding through the nozzle to a sufficiently low temperature so that ice formation of the liquid droplets could be achieved and its effectiveness could be examined. This required that the stagnation pressure driving the flow be close to 2000 psig prior to pressure regulation. Therefore, a high pressure Baur U-E3 air compressor has been

Figure 3 Detailed Schematic Diagram of High Speed Jet Impingement Facility.



Parts List for Figure 3.

Parts List

1	Compressor:	Bauer, Utilus, 3Hp, 5000 psig @ 3.4 SCFM, Model B0032DLF2AM02, SN 95X06217
2	Air/Water line:	Supreme SMLS 3/8" Stainless and 1/4" Brass insulated with Fiber glass pipe insulation
3	Air Tanks:	Superior, Ten 40 liter, 2500 psig
4	Valves:	Whitey, SS-63TF8, 1/2", 2500 psig
5	Regulator:	Tescom 500, 3000/600 psig
6	Heaters:	Two 3000W Coil Heaters
7	Insulation, Heater:	Calcium Silicate, 1 1/2" thick, 1 3/8" ID
8	Valves:	Whitey, SS-63TF8, 1/2", 2500 psig
9	Pressure Transducer:	Viatran, 0 - 500 psig, Model 3415AU2AAA20, SN 13291699
10	Thermocouples:	J-Type
11	Differential Pressure:	Validyne, Model DP215-40, SN 23872
12	Air Velocity:	Annubar
13	Water Tank:	Stainless Steel, One Gallon
14	Water Heating Element:	240W, 220V
15	Valves:	Whitey, SS-63TF8, 1/2", 2500 psig
16	Thermocouples:	J-Type
17	Mixing Chamber	Stainless Steel, 0.0045" water inlet hole
18	Thermocouples:	J-Type
19	Thermocouples:	J-Type
20	Nozzle:	Conventional or Annular converging/diverging nozzle
21	Power Regulator (Heaters):	IMS, Model 2, SN 1498, 240V, 20A

Not Shown:

Scale:	Ohaus Analytical Standard, AS200, +/- .1mg, SN # 2745, UF 4910-AA-133267
Laser:	Omnichrome, Model 532, SN # 4080, Max output 11 mW
Laser Power Supply:	Omnichrome, Model 150, 110V
Power Meter:	Newport Power Meter, Model 1818-C, 20mW setting, UF 4910-AA-125750
Eye:	Newport, Model 818-SL, SN 4590, Washer with 1/2" ID to restrict light input
Computer:	Northgate Computer Systems, 286, UF 4910-AA-107694

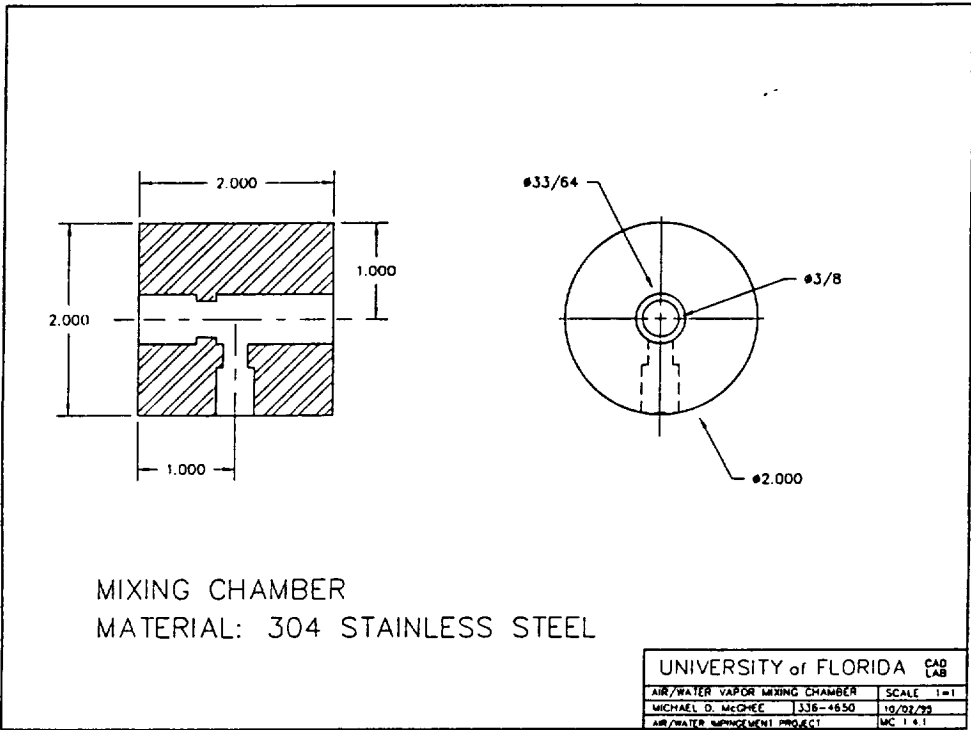
installed to charge ten 40 liter k-bottles which have been installed in parallel. The specifications of the compressor are as follows: 3.5 cfm delivery rate, 5000 psig maximum pressure, with 3 intercooled stages driven by a 3 HP motor at 3460 rpm. The compressor charges the ten 40 l k-bottles to 2000 psig in approximately two and a half hours. Although the k-bottles are rated to 2500 psig, a relief valve has been installed and set at 2000 psig. A pressure regulator is placed at the discharge of the k-bottles. Typically, the regulator is set to 320 psig to achieve the desired air flow rate.

Downstream of the pressure regulators is a 6 kW air heater section. Two 3 kW band heaters firmly fit around the outside of a 7/8" O.D. copper tube. The band heaters are insulated with 1½" calcium silicate insulation. Thermocouples are installed at the inlet and discharge of the heater section. All thermocouples used in the test facility are type J. The power to the band heaters are controlled with a pulsed output 240 VAC PID temperature controller. When full power is required, a thermocouple attached to the copper heating section is used for feedback to the temperature controller so that the copper heater section does not melt.

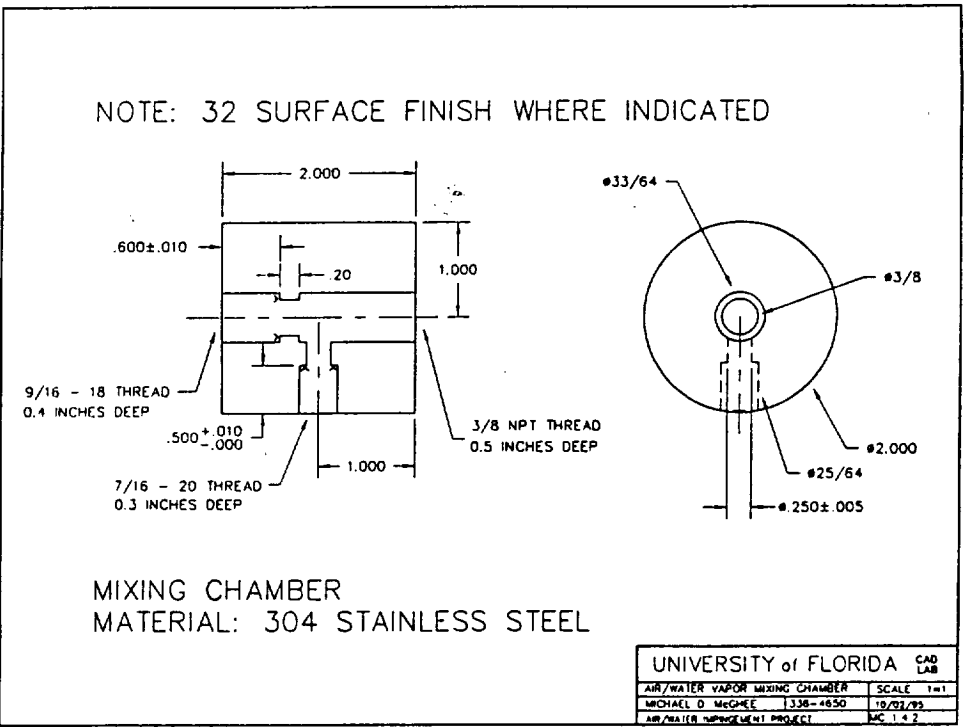
The air exiting the air heater section passes through an Annubar type flow meter. Downstream of the flow meter is the air/water mixing chamber. In addition to mixing the air and water, the mixing chamber provides precise metering of the water flow. The design of the mixing chamber is shown in Figures 4a-d. Two different sized orifices are inserted into the mixing chamber. The 3/8" orifice adapter is inserted into the air side of the chamber and is used to accelerate the air flow through the chamber. The pressure in the chamber drops as the air is accelerated which allows the pressurized water to flow into the

Figures 4a-d Detailed Drawings of Mixing Chamber and Orifice Adapters.

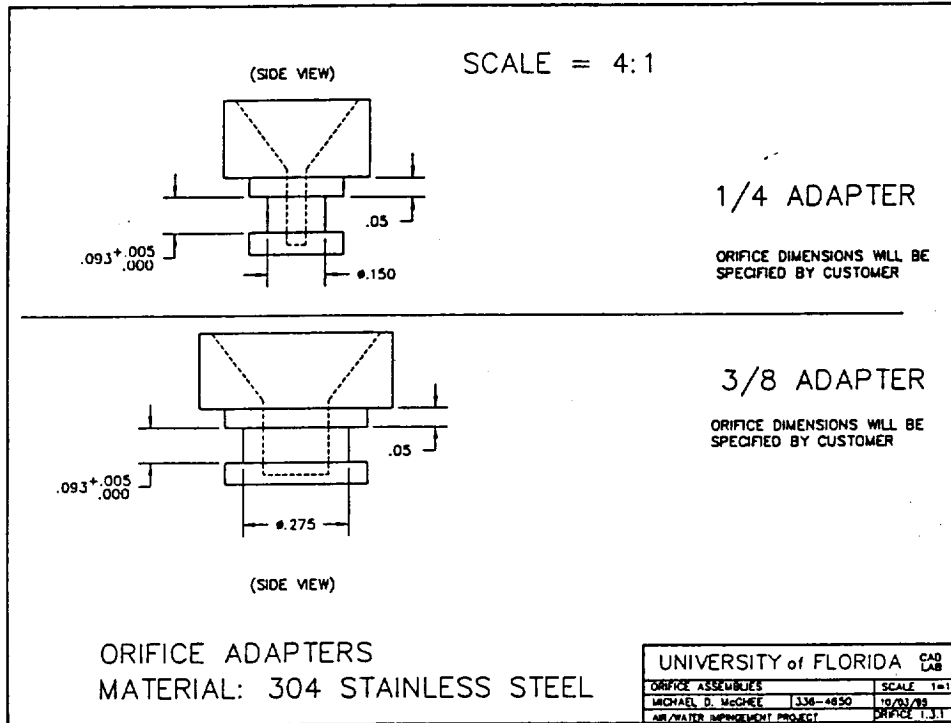
4a



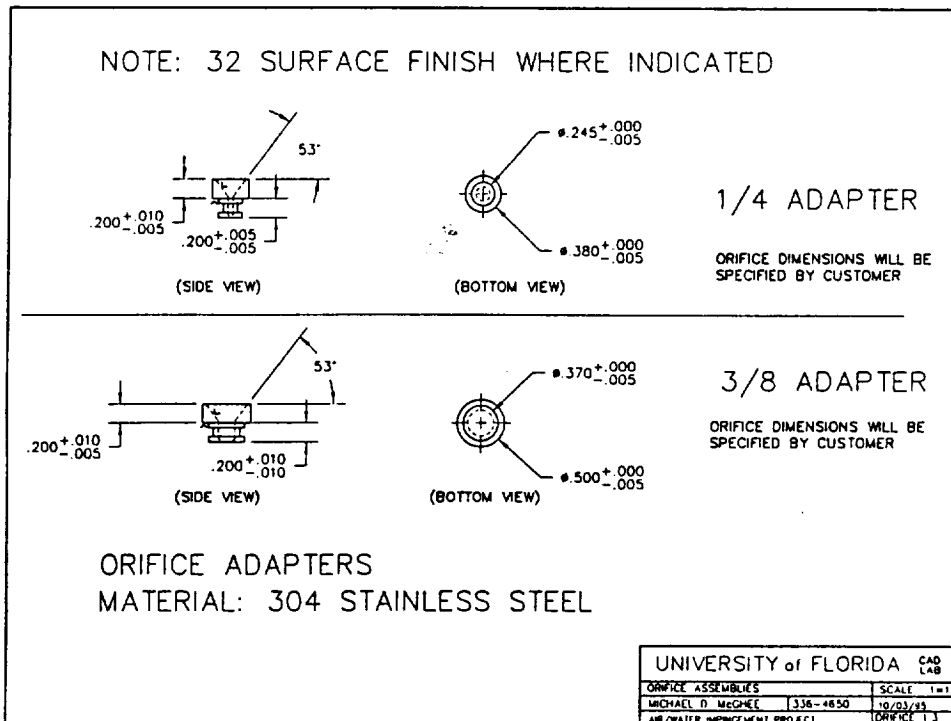
4b



4c



4d



chamber. The water flow rate is metered with the 1/4" orifice adapter. The orifice diameter for the air side is 0.195 inches and the orifice diameter for the water side ranges from 0.013-0.020 inches, depending on the desired water flow rate.

The water side of the jet impingement cleaning facility primarily consists of a high pressure stainless steel cylinder which sits inside a water bath. The cylinder is rated for 5000 psig and has a capacity of 1 gallon. Distilled water is placed inside the cylinder, and it is pressurized with air downstream of the heater section. It is very important that liquids with no contaminants are placed inside the water cylinder because even the smallest contaminants can plug the water side orifice. The water cylinder is mounted inside a water bath which is open to the atmosphere. The water bath can be heated or cooled in order to control the water temperature inside the cylinder.

The high pressure two-phase mixture exiting the mixing chamber is connected to a high pressure stainless steel hose. A converging-diverging nozzle is fitted at the end of the hose. The exit area to throat area ratio of the nozzles considered in this study is 5.44 which corresponds to a design discharge Mach number of 3.14. Two different nozzle designs were considered in this study, both of which were designed and manufactured at NASA KSC. A conventional converging-diverging nozzle is shown in Figure 5a and an annular type converging-diverging nozzle is shown in Figure 5b. Due to two-dimensional flow behavior in the nozzle the two-phase jet discharging the conventional nozzle diverges thus creating a wider jet with smaller concentration of liquid droplets at the cleaning surface. The two-phase jet in the annular nozzle converges at the exit. Thus the jet diameter is narrower and the concentration of droplets at the target surface is higher. Although the conventional

Figure 5a Conventional Converging-Diverging Nozzle.

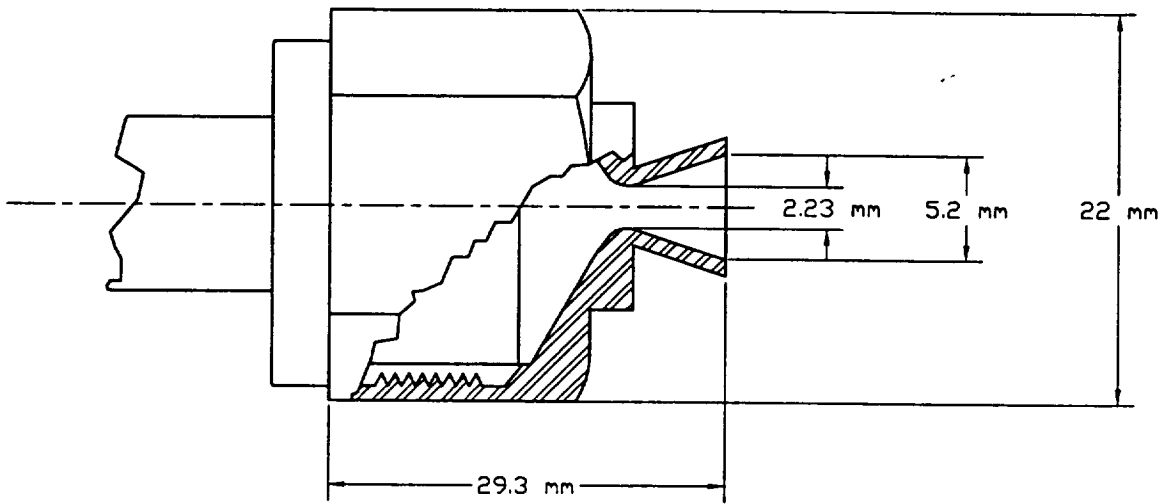
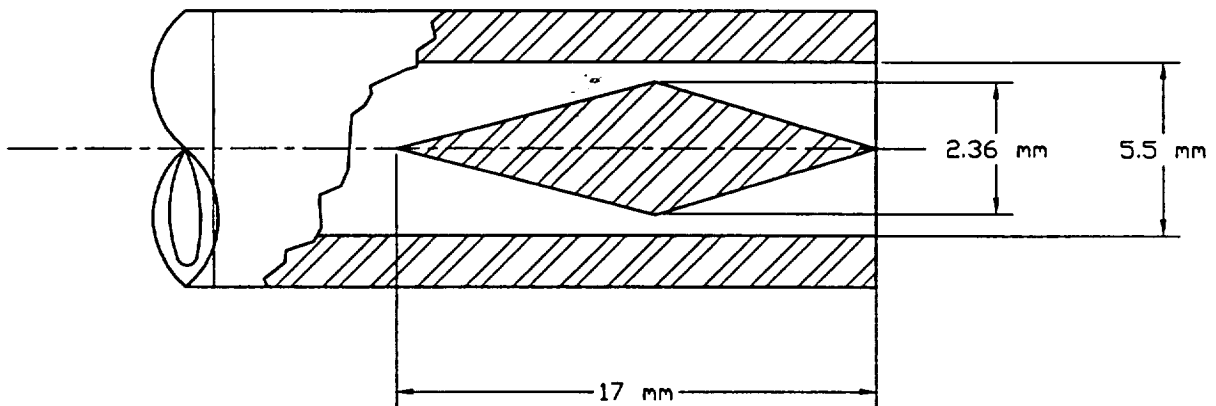


Figure 5b Annular Converging-Diverging Nozzle



nozzle can cover a greater surface area than the annular nozzle, it remains for experimental verification which nozzle can remove the greatest amount of nonvolatile residue.

3.2 Description of Instrumentation

Type J thermocouples are placed at various locations throughout the jet impingement facility to measure temperature. The most important temperature measurements required to interpret the experimental results are the air temperature exiting the heater section, the air temperature entering the annubar flow meter, the water temperature entering the mixing chamber, and the mixture temperature discharging the mixing chamber. During later experiments it was observed that when the two-phase mixture was heated, the mixture temperature entering the nozzle was significantly less than that discharging the mixing chamber due to heat transfer losses from the stainless steel high pressure hose. In subsequent tests, the hose was insulated, and a thermocouple was inserted just prior to the entrance of the nozzle to measure the mixture temperature.

The static pressure of the air at the discharge of the heater section and just before the annubar flow meter is measured with a Viatran 3400 series strain gage type transducer with a pressure range of 0-500 psig and a proportional current output. The air pressure discharging the k-bottles is regulated with a Tescom 500 3000/600 psig pressure regulator.

The air flow rate is measured with a 1/2" annubar flow meter manufactured by Dietrich Standard. The pressure drop across the annubar is measured with a Validyne DP215 magnetic reluctance differential pressure transducer. The Validyne transducer signal is conditioned with a CD15 carrier demodulator and has been calibrated for a range of -5 to

5 psid which corresponds to a linear output ranging from -10 to 10 Vdc. The water flow rate is measured using the catch and weigh method. An Ohaus AS200 precision balance is used to measure the water sample.

A laser reflectivity method has been developed for measuring the quantity of residue on the cleaning surface; see next section for details. Figure 6 shows a schematic diagram of the measuring technique. A 100 mW argon-ion laser is used to illuminate the cleaning surface. Typically, the laser is set at its minimum output, 11 mW. A Newport 818-SL power meter is used to measure the spectral directional reflectivity. The spectral directional reflectivity is a function of the quantity of residue on the cleaning surface.

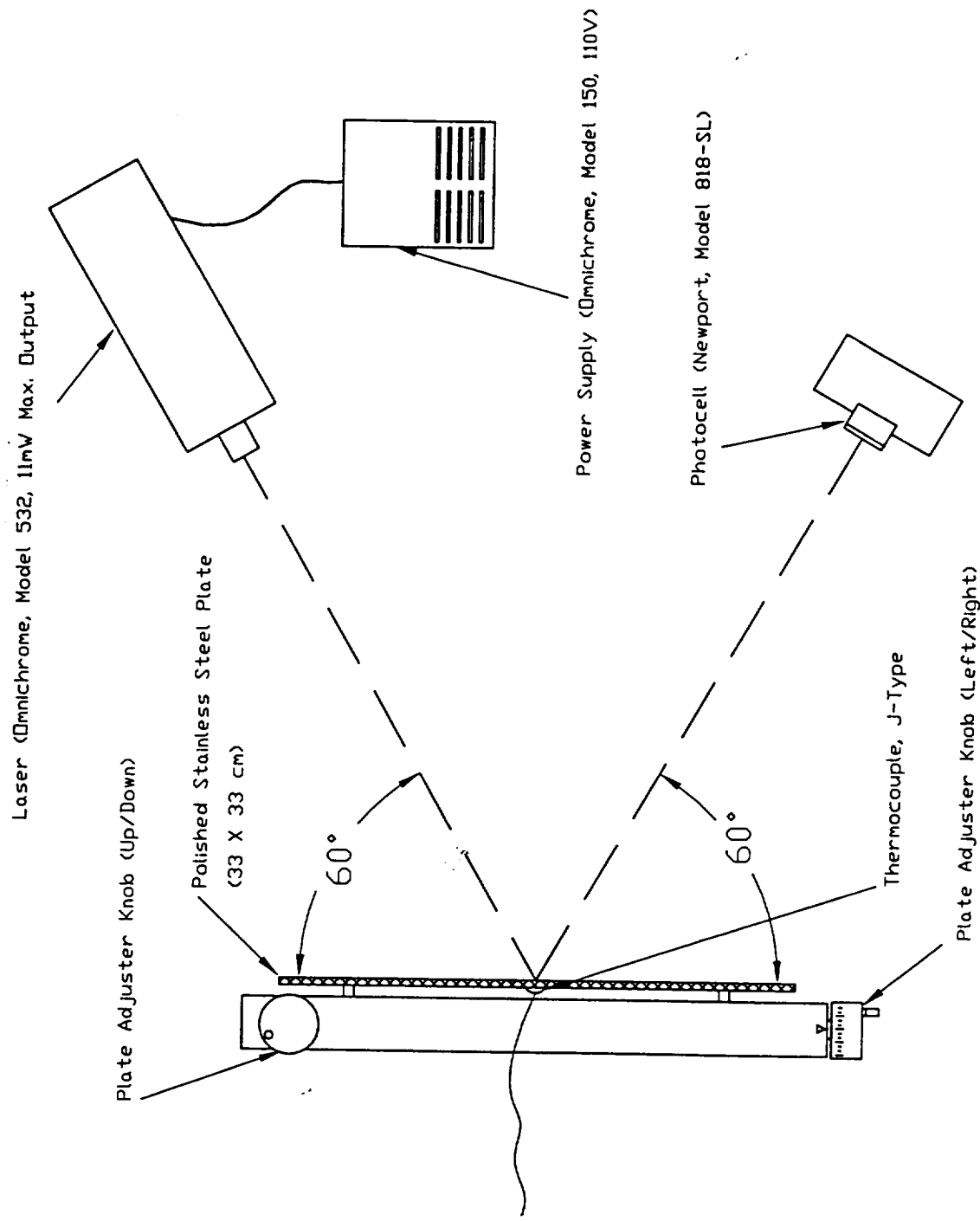
The output from all instrumentation is measured with an Access 12 bit analog to digital converter which is mounted inside a PC style microcomputer. A 16 channel multiplexer with programmable gain is interfaced with the analog to digital converter. Various algorithms used to control the data collection and analysis were programmed in Quick Basic.

3.3 Reflectivity Calibration and Residue Measurement Protocol

The following describes the procedure of the reflectivity method for measuring and calibrating the quantity of contaminant on the cleaning surface as a function of the reflectivity. The cleaning surface used for all tests consists of a polished 30 x 30 cm stainless steel plate. The laser, power meter, and cleaning surface are to be aligned as shown in Figure 6.

A) Turn on laser, scale, power meter, and computer. Allow 20 minutes for the laser

Figure 6 Experimental Alignment for Laser Reflectivity Residue Measurement.



to reach steady-state power output prior to any testing.

B) Remove all objects from the bench on which the scale rests, and do not lean on the bench. Use dial pegs located at the front of the balance in order to level it. The level indicator is located at the back of the balance.

C) Place the spatula on the balance and wait for the reading to stabilize.

1. Prior to attempting a reading, turn off the air conditioning, compressor, and any other vibrating or blowing equipment. The air disturbance or vibrations could adversely influence the measurements.

2. Do not lean on the table or create air currents by walking or breathing in the vicinity of the measurement area.

3. When placing items on the balance, do so as consistently as possible. Rotating the tray can cause fluctuations in the mass measurements.

D) Tare the balance.

E) Squeeze a small amount of grease out of the tube onto a paper towel to ensure consistency of the grease sample.

F) Apply a grease sample to the spatula.

G) Record the mass of grease.

H) Lightly dab grease on the cleaning surface. Try to dab grease evenly over the entire surface. Use a coarse grid pattern, filling in vacant areas. Dab until grease no longer comes off the spatula. Try to remove grease from the heavier dabs and spread to the lighter coated areas.

I) Now spread the grease evenly over the entire surface using a small circular motion.

Use a heated blow dryer for ease of spreading. Do not apply heat directly to the spatula.

This procedure will insure that the grease is uniformly spread over the cleaning surface.

J) Place the spatula back on the balance, close the balance doors and allow to cool.

Do not record the balance reading yet.

K) Heat affects the reflective properties of the grease. Therefore, use pressurized air (200-400 psig) to cool the back of the plate to approximately 30°C. This may require up to 5 minutes, depending on the extent to which the plate was heated. At this stage, cleaning or calibration takes place. If the plate is to be cleaned, place the cleaning surface on its stand and follow the cleaning procedure outlined in Section 3.4. Once the surface is cleaned continue to step L. If calibrating, continue directly to step L without going through the cleaning process.

L) Run the computer program "laser.exe" and follow prompts, entering all information requested.

1. When asked to calibrate the meter for initial power readings, turn the Newport power meter down to its finest setting and zero the meter to ambient light conditions. Return the meter to the 20 mW setting. Place the light receiver over the laser outlet and hit the enter button.

2. When cued to return the eye, move the light receiver stand to the position outlined on the bench. Insure that the entire beam enters the eye. A small percentage of light will reflect back out of the eye. By directing this light directly back at the spot which the laser plate is striking ensures that the laser beam is striking normally to the receiver surface.

3. "Laser" will give a prompt to "Hit 2 to finish sampling."

4. The plate is moved by turning either a horizontal for vertical positioning dial. By hitting "Enter" each time the horizontal positioning dial is turned, samples of the power meter output are collected. This is repeated for 52 horizontal positions. The vertical positioning dial is then turned eleven times, and another string of horizontal data is collected. The process continues until six rows have been collected. Each time "Enter" is depressed, power meter samples are collected at 10 Hz and the average power reading is displayed. After these data have been collected, "2" is depressed on the computer.

5. The computer program will give a prompt to test the output power of the laser again, and will then collect information regarding the test.

6. A final output screen will consolidate all the important information and ask whether or not the data should be saved to a file. If yes, the data is stored to a file named by the current date and time (i.e. 5131641.dat is May 13, 4:41 pm).

7. A hard copy of the data can be obtained using the "print screen" key.

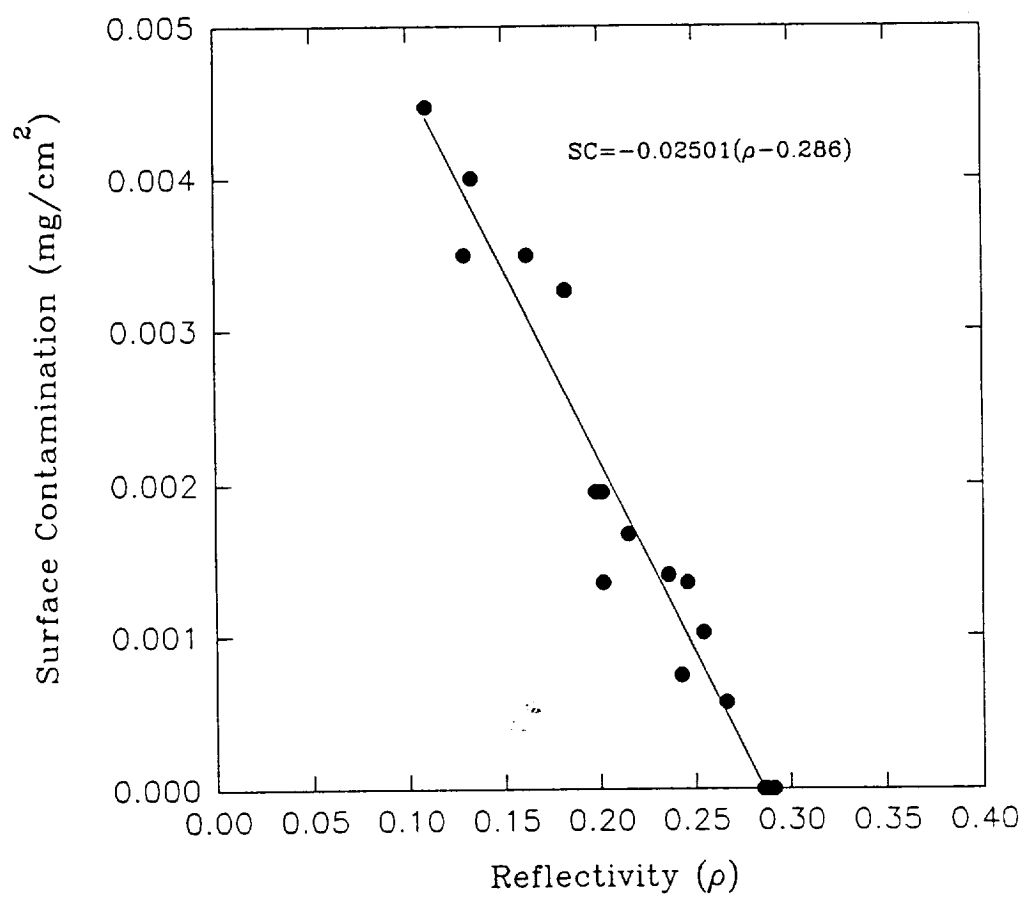
M) Once the tests are completed, methyl alcohol is applied to a paper towel, which is used to remove the grease from the test surface.

All of the cleaning tests carried out in this investigation used Dow Corning 55 (DC-55) O-Ring Lubricant as the surface residue. Figure 7 shows a calibration curve for the DC-55 residue contaminant level as a function of the laser reflectivity at 60° incident angle.

3.4 Protocol for Operating High Speed Jet Impingement Facility

The following explains the detailed protocol for experimental cleaning investigations using the high speed jet impingement facility.

Figure 7 Calibration Curve for Residue Contamination Using Laser Reflectivity.



- A) Close all system valves.
- B) Open all valves on air storage tanks.
- C) Turn on the compressor only if tanks require charging.
- D) Turn on the water bath heater and allow the water to reach the desired temperature only for experiments in which water heating is required.
- E) Turn on the IMS power regulator and warm the air heating elements to 540°F only for experiments in which air heating is required.
- F) Turn on the computer, Viatran pressure transducer power supply, Validyne differential pressure transducer carrier demodulator, Newport power meter, and the Ohaus electronic balance.
- G) Once the plate is prepared for cleaning (as per instructions in Section 3.3), transfer the stainless steel cleaning surface to the test stand.
- H) Select nozzle wand intended for cleaning. Using a ruler and protractor, attach a reference ruler to the nozzle. This ruler allows the operator to maintain a specified distance from the cleaning surface and control the approach angle of the jet with respect to the cleaning surface.
- I) Run the computer program "csn.exe." The program will cue the operator to zero the Validyne transducer (insure that there is no fluid flow at the time of zeroing). The program provides a means of real time monitoring of system instrumentation.
- J) Open the valves just prior to the pressure regulator and downstream of the heater section.

K) Adjust the pressure regulator to approximately 50 psig and allow air to discharge from the system for three minutes. This allows the system to achieve a steady-state temperature.

L) Adjust pressure regulator for 320 psig output, and open the water valve just prior to the mixing chamber. The nozzle operator (NzOp) is cued by the system operator (SyOp) to begin cleaning. The SyOp monitors a predetermined cleaning time and records system information via "csn.exe". The NzOp cleans the test surface using up and down motions, starting at one side and blowing the grease away from the initial location.

M) After the NzOp is cued by the SyOp to stop cleaning, the water valve is closed.

N) Adjust the pressure regulator to 0 psig output.

O) Dry test surface using pressurized air (100 psig).

P) Place test plate on the laser calibration and verification stand and follow the procedures outlined in Section 3.3 to measure the surface residue remaining on the plate following cleaning. If no further testing is desired, follow the steps below to shut down the system.

Q) Close all system valves.

R) Close all valves on air storage tanks.

S) Turn off the compressor once tanks are charged to desired level.

T) Turn off the water bath heater.

U) Turn off the IMS power regulator.

V) Turn off the computer, Viatran pressure transducer power supply, Validyne differential pressure transducer carrier demodulator, Newport power meter, and the Ohaus

electronic balance.

4 Experimental Results

A series of cleaning tests were conducted in order to study the system performance as different operating parameters were varied. The system performance is characterized by the rate of contaminant removal. As mentioned previously, Dow Corning 55 (DC-55) O-Ring Lubricant is used as the surface residue for all tests conducted. All of the test results are summarized in Table 1.

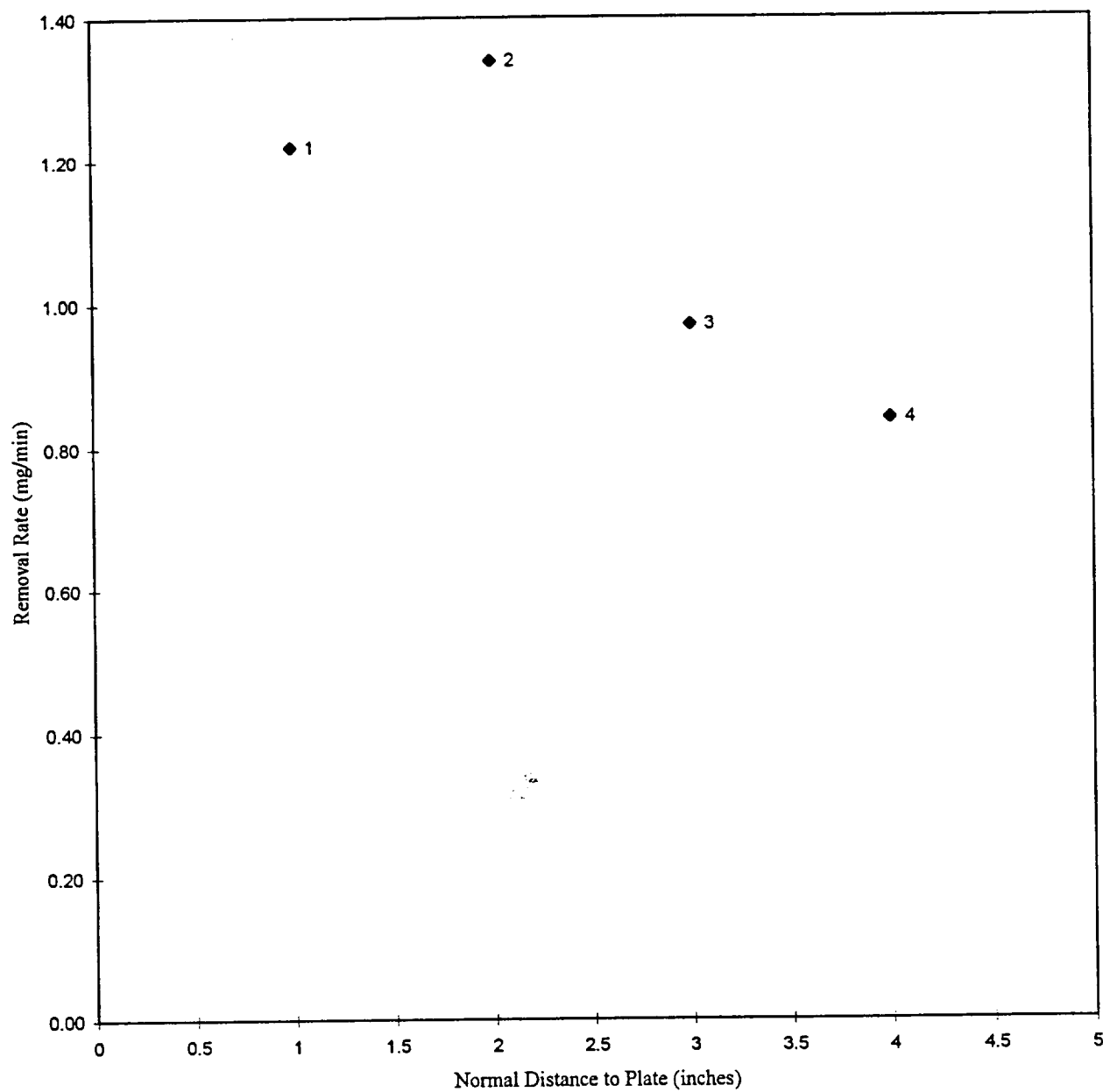
During the initial testing stages of the facility, a series of preliminary tests were conducted using the conventional converging-diverging nozzle, which are not documented in Table 1. The air and water temperatures were not controlled while the jet approach angle with respect to the cleaning surface was varied during those preliminary tests, and it was found that an approach angle of approximately 15° yielded the best performance. As the angle approached 90° , the two-phase jet was ineffective in removing residue from the cleaning surface. Thus, for all subsequent tests which are reported in Table 1, the nozzle approach angle was maintained at 15° . Several tests were also conducted in which ice formation of the droplets from the nozzle were noted, and it was observed that the ice impacting the surface was ineffective in removing residue. Thus for all subsequent tests, ice formation was avoided. The fact that the abrasive impact of the ice is ineffective in removing residue is in agreement with the observation of Hills (1995) in which a CO_2 jet spray was tested.

The fact that an approach angle of 90° is ineffective for removing residue while 15°

is most effective is also an expected result, especially when considering the experience gained from particle impact erosion. Particle impact erosion studies have shown that the cutting action of solid particles shearing the surface is most effective in eroding a target surface. When the impact angle of the particles is 90° the particles do not shear the surface, but rather work harden the surface. The surface will eventually fail due to brittle fatigue. When the particles impact the target surface at 15° - 20° the shearing energy is high and the maximum erosion rate is obtained. Similarly, when liquid droplets impact a residue, the shearing force is most effective in breaking the cohesive bonds between adjacent residue molecules. A normal force or impact will tend to penetrate the residue and displace it to the side and will not be effective in breaking cohesive bonds. Thus the observed result that a 15° approach angle results in the highest rate of residue removal is consistent with theoretical considerations.

During the first four tests summarized in Table 1, the conventional converging-diverging nozzle was used and its distance from the cleaning surface was varied from 1-4 inches. It was found that the best performance is observed for a distance of 2 inches, although the result is not significantly different from the 1 inch test. The trend of rate of contaminant removal as a function of nozzle distance is shown in Figure 8. The further the nozzle is from the surface, the droplet concentration impacting the surface is reduced. Also due to viscous drag, the droplet velocity impacting the surface is be reduced. It is believed that both these factors contribute to a reduction in residue removal rate with increasing nozzle distance. Test number 5 was also performed with a nozzle distance of 2 inches, but since the source pressure from the cylinders was low (850 psig) and the water was heated,

Figure 8 Residue Removal Rate as a Function of Nozzle Distance to Cleaning Surface (Conventional Converging-Diverging Nozzle, 15° Approach Angle, No Heating).



the mixture temperature was high (24.6° C) compared with the previous tests. It is seen an increase in the mixture temperature resulted in a significant increase in the rate of contaminant removal.

Tests 6,7,8, and 10 tested the rate of contaminant removal as a function of nozzle distance using the annular nozzle. Figure 9 summarizes the results from these tests. The closest distance to the cleaning surface tested was 1.0 inch, and it is observed the removal rate sharply declines with increasing distance from the cleaning surface. Also, it is noted that the cleaning performance of the annular nozzle is significantly better than that of the conventional converging-diverging nozzle. Thus for all subsequent tests the annular nozzle performance is tested. Tests 8 and 9 were conducted with the same nozzle distance from the cleaning surface, but the mixture temperature for test 9 was about 9°C greater than that for test 8. With only 9° increase in the mixture temperature, and the rate of residue removal increased by about a factor of 6.

Since the mixture temperature has such a large influence on the residue removal rate, a number of tests were carried out to explore the temperature influence. Tests 13-20 explored the influence of increasing the water temperature without controlling the air temperature. These results are summarized in Figure 10. The data show that the rate of residue removal increases slightly with increasing water temperature. However, it is observed that the mixture temperature also increases, and the increase in the residue removal rate is primarily due to the increase in the mixture temperature. Because the mass flow rate of air is so much greater than water, controlling the air temperature has a much more significant impact on the mixture temperature.

Figure 9 Residue Removal Rate as a Function of Nozzle Distance to Cleaning Surface (Annular Converging-Diverging Nozzle, 15° Approach Angle, No Heating).

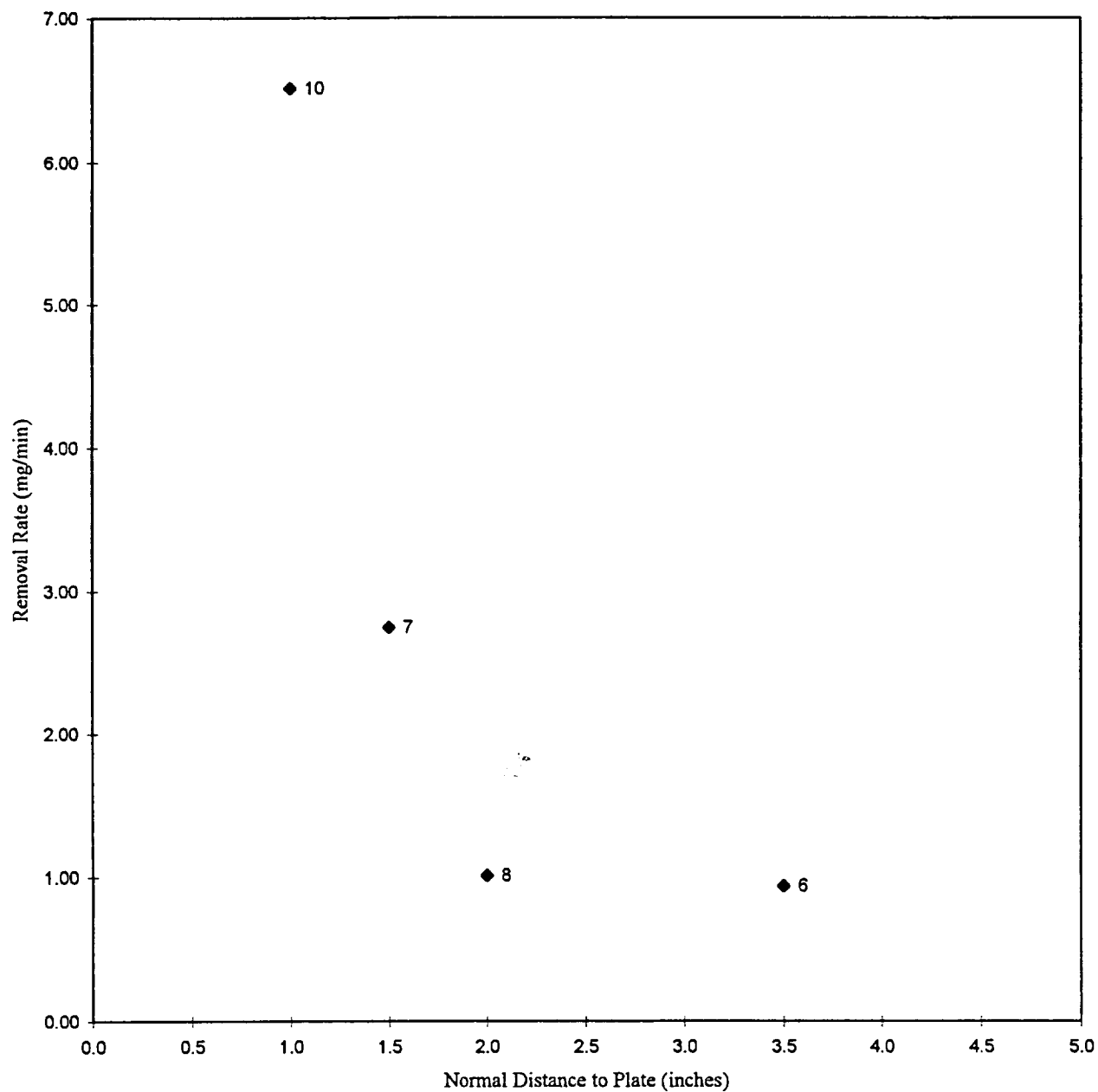
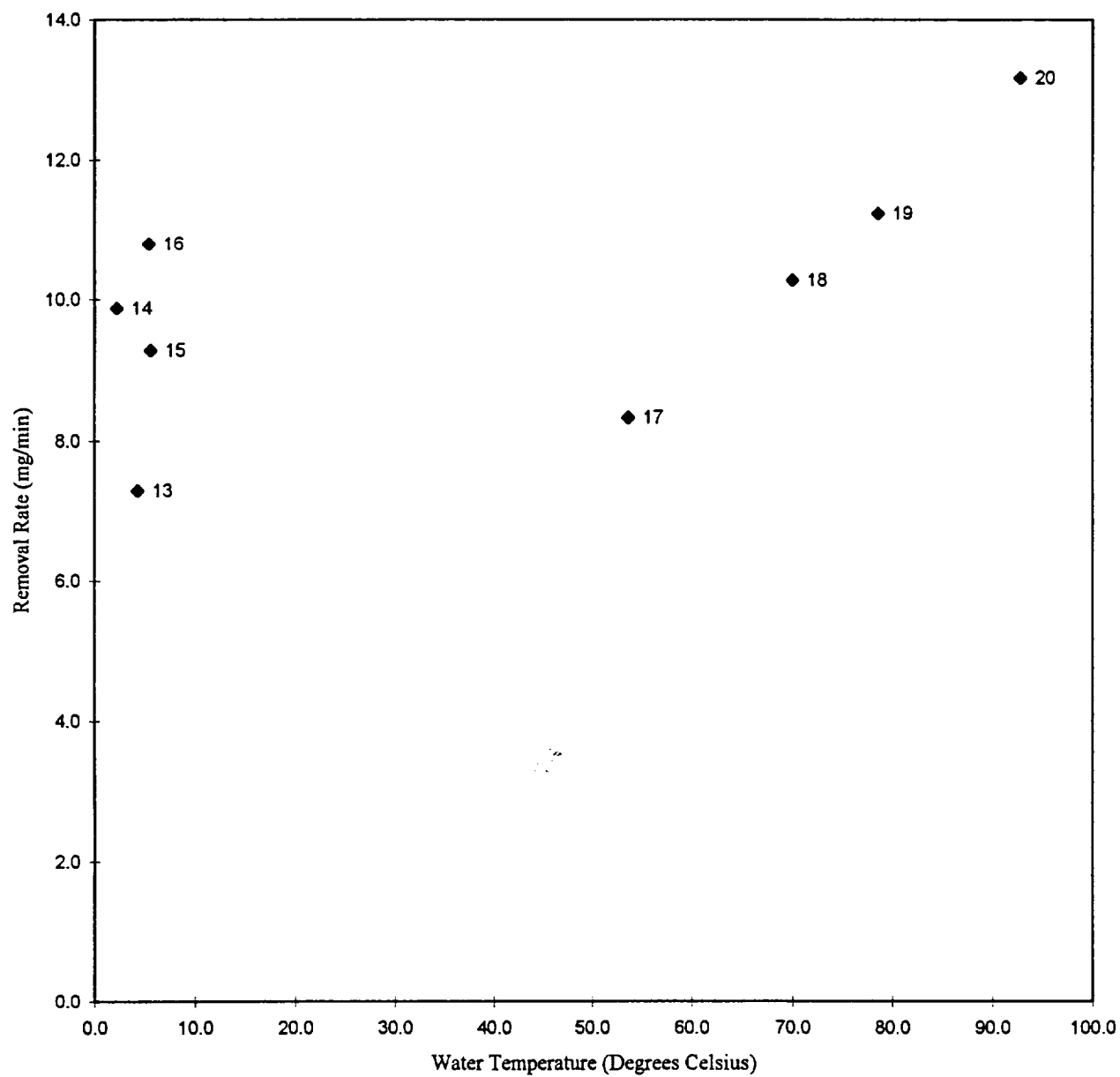


Figure 10 Residue Removal Rate as a Function of Water Temperature
(Annular Converging-Diverging Nozzle, 15° Approach
Angle, 1" Nozzle Distance).



For tests 21-29, the distance of the jet nozzle from the cleaning surface as well as the air and water temperatures were varied. The water flow rate for tests 21-29 is approximately 20 mg/min, which is about half that recorded for previous tests. Although it was not known at the time, the water flow rate was reduced due to thermal expansion of the aluminum water orifice. The thermal expansion resulted in a reduction in the orifice area. Also, it must be noted that the mixing temperature for these tests is not representative of the mixture temperature entering the nozzle. This is because the mixture temperature is measured prior to entering the stainless steel hose to which the nozzle is connected. There is significant heat loss from the hose to the surroundings, and during tests 21-29 the hose was not insulated. These test results demonstrate that a nozzle distance from the cleaning surface of 0.75 inches results in enhanced residue removal when compared to a nozzle distance of 1 inch. Poorer performance is realized at a nozzle distance of 1.5 inches. It is also learned from these tests that the rate of residue removal increases with an increasing mixture temperature. In tests 21-25, although the mixture temperature does not show significant variation, the outlet temperature of the mixture from the nozzle was increasing because the stainless steel hose, which has a large thermal capacity, continually increased in temperature the longer the facility was operated. Thus the heat loss was reduced and the mixture temperature exiting the nozzle increased.

During tests 30-40, a larger orifice was installed to increase the flow rate, and the stainless steel hose was insulated. When the results of tests 21-25 are compared with those of tests 30-40, it can be observed that the larger mass flow rate of water results in enhanced rate of residue removal. This is consistent with theoretical considerations discussed in

Section 2.3.

Figure 11 summarizes the rate of removal as a function of mixture temperature.

First, it is worth noting that the mixture temperature has the most significant influence on the rate of residue removal. As the mixture temperature is increased, there is a sharp increase in the residue removal rate. As the mixture temperature is further increased, the residue removal rate drops off. In order to understand this trend, consideration is given to Eq. (4). The residue removal rate is inversely proportional to the interfacial tension between water and residue. The interfacial tension decreases with increasing temperature and thus the residue removal rate is increased. During these tests it was not realized that the mass flow rate of water was falling with increasing mixture temperature due to thermal expansion of the water metering orifice. Figure 12 shows the mass flow rate of water as a function of the mixing chamber temperature with a 0.016 inch water metering orifice installed. Thus as the mixing chamber temperature increased, the reduction in water flow rate offset the drop in interfacial tension.

The residue removal trends observed in this experimental investigation are consistent with the hypothesis that the dominant residue removal mechanism is due to emulsification of the residue in the liquid.

These results suggest that the optimum system performance can be realized by using the annular nozzle with an approach angle of 15 degrees with respect to the cleaning surface at a distance from the cleaning surface of 0.75 inches with as high a mixture temperature as possible without evaporating the water. It is further noted that the system piping and hose line should be well insulated to maintain a higher mixture temperature. Increasing the water

Figure 11 Residue Removal Rate as a Function of Mixture Temperature
(Annular Converging-Diverging Nozzle, 15° Approach
Angle, 3/4" Nozzle Distance).

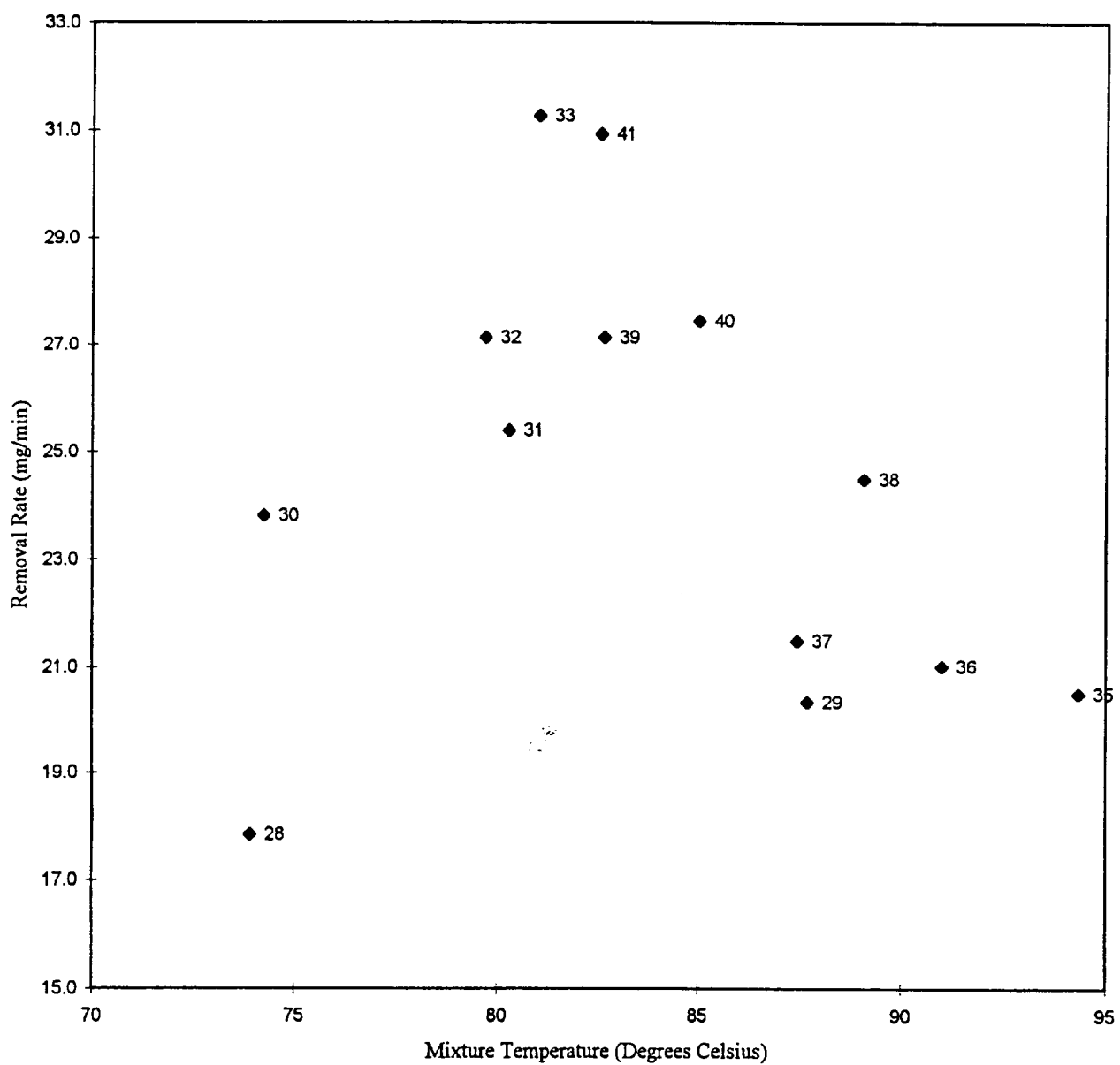
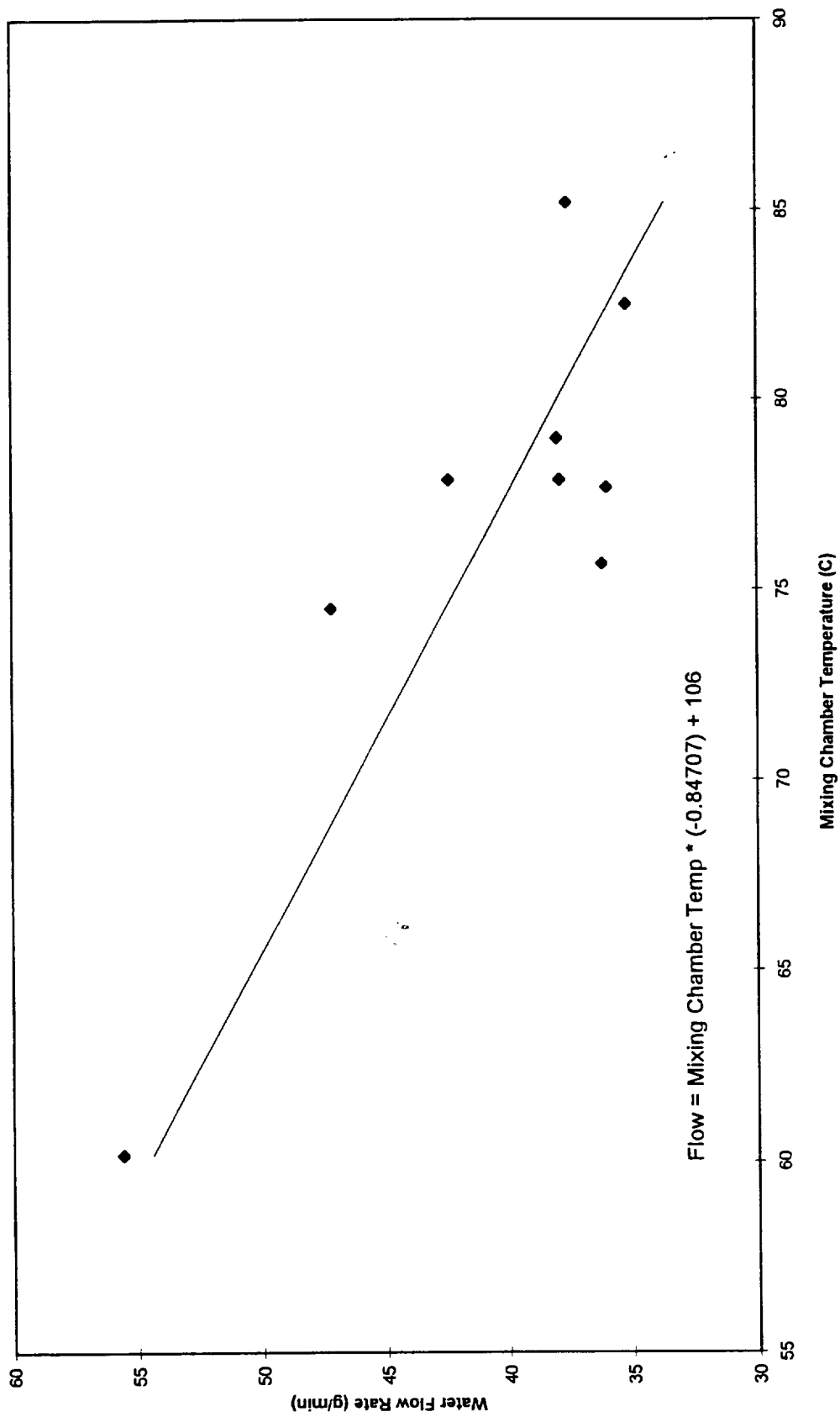


Figure 12 Water Flow Rate as a Function of Mixing Chamber Temperature (0.016" Orifice).



flow rate increases the rate of residue removal. Thus the orifice size in the mixing chamber should be adjusted to obtain as high a water flow rate that is acceptable for cleaning and verification operations.

5 Conclusions

- i) A high speed jet impingement cleaning facility has been developed to study the effectiveness of the nonvolatile residue removal. The facility includes a high pressure air compressor which charges the k-bottles to supply high pressure air, an air heating section to vary the temperature of the high pressure air, an air-water mixing chamber to meter the water flow and generate small size droplets, and a converging- diverging nozzle to deliver the supersonic air-droplet mixture flow to the cleaning surface. To reliably quantify the cleanliness of the surface, a simple procedure for measurement and calibration is developed to relate the amount of the residue on the surface to the relative change in the reflectivity between a clean surface and the greased surface. This calibration procedure is economical, simple, reliable, and robust.
- ii) A theoretical framework is developed to provide qualitative guidance for the design of the tests and interpretation of the experimental results. The removal rate is proportional to the mass flow rate of the square of the droplet impact velocity. It increases with the decrease of the cohesive bond among the residue. The results documented in this report support the theoretical considerations.

iii) It is found that the jet approach angle of about 15 degrees results in most effective residue removal from the surface, a result very similar to the particle impact erosion of ductile materials. An incident angle of 90 degrees (normal to the surface) results in the most ineffective cleaning.

iv) The effect of temperature was examined in detail. In particular, it is demonstrated that the formation of ice at low temperatures actually results in lower removal rate of the grease contaminant comparing with the test results obtained at a higher temperature without ice formation. Further increasing in the mixture temperature significantly enhances the removal rate due to the weakened bond among residues at a higher temperature.

v) The performance of two nozzle geometries is compared. The annular geometry performs significantly better than the conventional converging-diverging nozzle under the same operating conditions. The reason is that the two-phase mixture jet exiting the conventional nozzle diverges which results in a wider jet that reduces the jet velocity. In the annular nozzle, the mixture moves toward the centerline of the nozzle prior to exiting. This delays the eventual spreading of the jet so that the decay of the jet velocity is slower in comparison with the conventional nozzle.

vi) For the annular nozzle operating at a nominal exit Mach number 3.14, the closer the distance between the nozzle exit and the cleaning surface (down to 0.75 inches), the higher the removal rate. This is consistent with the fact the two-phase jet velocity decreases along

the flow direction. For the conventional converging-diverging nozzle, a local maximum in removal rate is achieved at a distance of 2 inches from the surface. This suggests that the supersonic jet flow may converge at that distance due to the interaction of the shock waves with surroundings. The difference in the behavior between the two nozzles (with and without local maximum removal rate for distances down to 0.75 inches) suggests a significant influence of the nozzle geometry (consequently the flow structure) on the cleaning effectiveness.

6 References

- Caimi, R.E., and Thaxton, E.T., 1993, "Supersonic Gas-Liquid Cleaning System," *Proceeding of the Technology 2003 Conference*.
- Dearing, W.L., Bales, L.D., Bassett, C.W., Caimi, R.E., Lafferty, G.M., Melton, G.S., Sorrell, D., and Thaxton, E.T., 1993, "Methods for Using Water Impingement in Lieu of Chlorofluorocarbon 113 for Determining the Non-Volatile Residue Level on Precision Cleaned Hardware," *Alternatives to Chlorofluorocarbon Fluids in the Cleaning of Oxygen and Aerospace Systems and Components*, ASTM STP 1181, pp. 37-48.
- Finnie, I., 1972, "Some Observations on the Erosion of Ductile Metals," *Wear*, Volume 19, pp. 81-90.
- Hills, M.M., 1995, "Carbon Dioxide Jet Spray Cleaning of Molecular Contaminants," *J. Vac. Sci. Technol. A* 13(1), Jan/Feb, pp. 30-35.
- Hoff, G., Langbein, G., and Rieger, H., 1967, "Material Destruction Due to Liquid Impact," in *Erosion by Cavitation or Impingement*, ASTM STP No. 408, pp. 42-69.
- Kim, K.H., and Chang, K.S., 1994, "Three-Dimensional Structure of a Supersonic Jet Impinging on an Inclined Plate," *J. of Spacecraft and Rockets*, Vol. 31, p. 778.
- Kolkman, H.J., 1993, "Performance of Gas Turbine Compressor Cleaners," *Journal of Engineering for Gas Turbines and Power*, Vol. 115, pp. 674-677.
- Lamont, P.J., and Hunt, B.L., 1980, "The Impingement of Under-Expanded, Axisymmetric Jets on Perpendicular and Inclined Plates," *J. Fluid Mechanics*, Vol. 100, p. 471.
- Littlefield, M.D., Melton, G.S., Caimi, R.E.B., and Thaxton, E.A., 1994, "Cleaning Verification by Air/Water Impingement," *Proceedings of the 1994 Precision Cleaning Conference*.
- Melton, G.S., Caimi, R., and Thaxton, E.A., 1993, "Determination of Non-Volatile Residue on Precision Cleaned Oxygen and Aerospace Systems and Components by Means of Water Impingement and Total Organic Carbon Analysis," *Proceedings of the 1993 International CFC and Halon Alternatives Conference*.
- Morkid, R., 1995, "3M Announces New Fluorinated Fluid Alternatives," *3M Specialty Fluids*, Vol. 1, No. 2, October Issue.
- Thom, M.A., 1995, "Removing Perfluorinated Polyether Greases," *Lubrication Engineering*, September Issue, pp. 726-731.

Tsuboi, N., Hayashi, A.K., Fujiwara, T., Arashi, K., and Kodama, M., 1991,
"Numerical Simulation of a Supersonic Jet Impingement on a Ground," *SAE Transactions*
paper 912014.

7 Nomenclature

a	radius
A	surface area
c_p	specific heat
k	thermal conductivity
\dot{m}	mass flow rate
t	time
T	temperature
U	nozzle exit velocity
V	volume
α	thermal diffusivity
ρ	density
σ_{lr}	liquid-residue surface tension
ϕ	energy utilization parameter

Subscripts

ℓ	liquid
p	particle
r	residue